

*Dorđe Miltenović*  
*Milan Tica*  
*Aleksandar Miltenović*  
*Milan Banić*  
*Srdan Živković*  
*Žarko Mišković*

ISSN 1333-1124  
eISSN 1849-1391

## **PITTING OF TOOTH FLANKS OF CROSSED HELICAL GEARS MADE OF SINTERED STEEL**

UDC 62-58:536.421.5:620.178

### **Summary**

Crossed helical gears are used in cars and in many household appliances. The trend towards increased comfort in motor vehicles has led to the utilisation of more than a hundred servo-drives in luxury class automobiles. Important advantages of crossed helical gears are their easy and inexpensive design, low noise performance and high gear ratio that can be realised in one step. Sintered steel is a material with very favourable properties for the manufacture of crossed helical gears. High demands are set on gears made from sintered steel regarding wear and pitting load capacity. This report shows the results of the investigation into pitting resistance of crossed helical gears made of iron-based sintered material Fe1.5Cr0.2Mo that has undergone additional treatment.

*Key words:*        *sintered steel, gears, transmission, pitting*

### **1. Introduction**

The process of developing sintered parts involves moulding various powders in specially designed moulds. Under the pressure of 800 N/mm<sup>2</sup> density of about 7.5 g/cm<sup>3</sup> is achieved. Subsequently, the still raw moulded parts are heat-treated in a flow furnace by applying the method of multi-step temperature ranges (heating, sintering, cooling). During the sintering process at the points where powder particles touch each other they begin to fuse, thus creating new crystals which amalgamate this heterogeneous powder mixture. The sintering process is ended with the cooling phase. The properties of sintered parts depend not only on the porosity of the material and the composition of alloying elements, but also on the final heat treatment. Sintered iron and steel can be thermally hardened, either directly or after carburization [1]. Gears made of sintered material with the porosity below 10% and with a suitable heat treatment have good resistance to wear and pitting.

The work by Wendt [2] is the first one focusing on the study of load capacity of helical gears with worm and pinion made with a combination of steel and sintered steel. The author worked on the load capacity of this material combination. As for sintered steel, he used

Fe1.5Mo0.3C with material density of 6.9 g/cm<sup>3</sup> and 7.2 g/cm<sup>3</sup>. The paper considered the damage from wear and pitting of tooth flanks.

The capacity of machine parts is limited by defects which lead to boundary conditions, i.e. their destruction. One of the frequent damages in such gears is pitting. The paper presents experimental research relating to the properties of sintered materials, as well as to the pitting of tooth flanks of crossed helical gears.

## 2. Chemical composition of sintered steel and material variants

The material combination of steel and sintered metal has been investigated only in few research projects. Researchers from the company Höganäs AB, Sweden [3] investigated sintered metals Astaloy Mo (Fe0.85Mo) and Astaloy CrL (Fe1.5Cr0.2Mo).

**Table 1** Chemical composition of sintered steel Fe1.5Cr0.2Mo (%)

element	C	Si	Mn	P	S	Cr	Ni	Mo	Cu
%	0.2522	0.0508	0.1614	0.009	0.0012	1.5166	0.026	0.2096	0.0666

The basic raw material for sintered steel is iron powder. Iron powder is mixed with different metal powders by applying special alloy mixing techniques. A homogeneous powder mixture is important for uniform cross-sectional properties within the part. Copper increases the strength and yield strength, but decreases the elongation at break. Nickel improves the strength and relieves the weldability. Carbon (graphite) in small amounts increases the strength and hardness and improves subsequent heat treatment. Phosphorus improves the strength and elongation, but causes high sintering shrinkage.

The chemical composition of the sintered steel is shown in Table 1. The basis for all tested materials is the iron-based powder Fe1.5Cr0.2Mo. The material variants are shown in Table 2. A detailed description of additional treatment methods is given in [4].

**Table 2** Material variants of sintered steel Fe1.5Cr0.2Mo

	Additional treatment	Density /g/cm <sup>3</sup>	Temperature of sintering /°C	Dimensional change A /%
S1	no additional treatment	7.50	1120	0.16
S2	case-hardening	7.49	1120	0.16
S3	case-hardening + shot peening	7.49	1120	0.16
S4	pyrohydrolysis	7.50	1120	0.16
S5	sinter-hardening	7.43	1120	0.16
S6	2% copper addition	7.43	1120	0.64

## 3. Material tests

In order to determine the properties of various material versions extensive material tests have been carried out. To determine the exact Hertz's surface pressure in the tooth contact, the E-modulus and Poisson's ratio are required [5]. These values can go as far as 0.2% of the compression limit determined in a compression test. The tensile test allows for the determination of 0.2% - yield strength and compression limit. It also determines the density of 10 wheels per batch.

### 3.1 Density of test gears

The measurement of density of helical gears is done according to the buoyancy method. By means of a hydrostatic balance one can determine the weight of helical gears in air  $m_L$  with the density  $\rho_s$ , as well as the weight in water  $m_w$  with the corresponding density of  $\rho_{Fl}$ .

The difference between the two weighings arises from the principle of Archimedes which states that the weight of the displaced fluid is directly proportional to the volume of the immersed body.[11, 12]

$$V_s = \frac{m_L - m_w}{\rho_{Fl}} \quad (1)$$

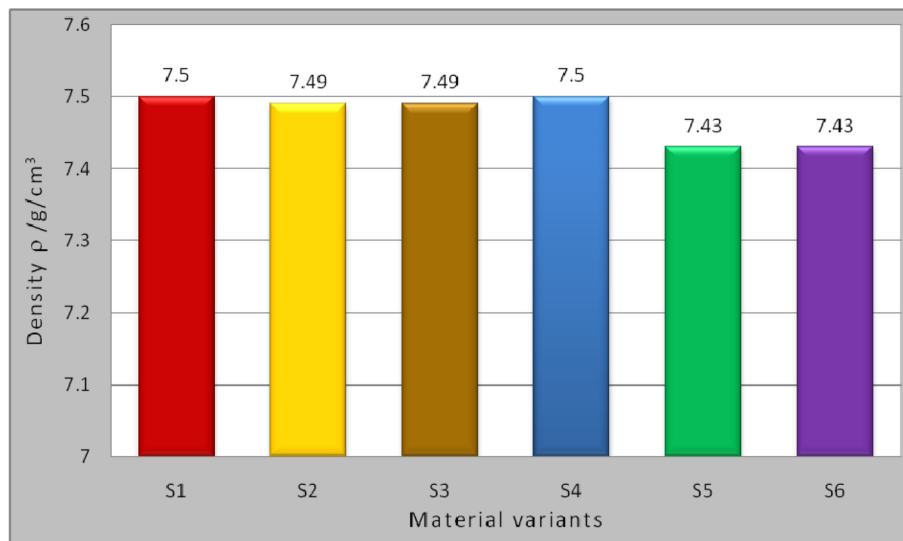


**Fig. 1** Comparison of the density of all material variants

The density of helical gears is calculated according to the following formula:

$$\rho_s = \frac{m_L}{m_L - m_w} \rho_{Fl} \quad (2)$$

The density specification for sintered helical gears made of the base material without undergoing any further treatment (S1) is 7.5 g/cm<sup>3</sup>. Figure 1 shows a comparison of density mean values for various types of helical gears.

The density of sintered helical gears is in accordance with the specified tolerance to the required density. For the hardened materials (S2), hardened and shot peened materials (S3) as well as for water vapour-treated materials (S4) the densities are approximately equal to those of the materials which have not undergone any additional treatment (S1) – 7.5 g/cm<sup>3</sup>. A slightly smaller density can be found with the sinter-hardened material and with the materials with 2% of copper addition. The alloying process in which 2% of copper is added to the base powder results in a lower density. This is due to the increase in the wheel size with the same amount of powder.

### 3.2 Hardness test

The micro-hardness of the gears is measured at nine locations which can be recognised in the arc shown in Figure 2. The Vickers hardness test HV0.1 is the test performed with a test load of 0.9807 N, which is common for such micro-hardness measurements. Figure 2 shows the arrangement of the measuring points. The preparation of cross-section samples is

performed by means of the wire electrical discharge machining (EDM) and a subsequent grinding, such as polishing treatment.

The micro-hardness profile of the gears is variable with respect to the tooth thickness. The largest micro-hardness is normally present at the edge regions of the layer hardened with martensite (Points 1 and 2).

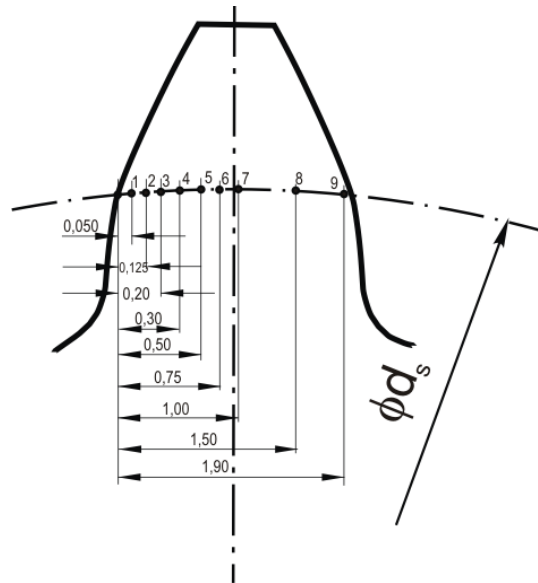


**Fig. 2** Positions of measuring points for micro-hardness, where  $d_s$  is pitch diameter

A comparison of micro-hardness measurements (mean values) of helical gears with different material variants is shown in Figure 3. As it might have been expected, the material variants with hardening or case-hardening and shot peening have the largest micro-hardness mean values. The smallest micro-hardness averages are found in the material variants that have not undergone any treatment or have undergone steam treatment. The micro-hardness profile of gears is variable with respect to the tooth thickness. The largest micro-hardness is normally present at the edge regions of the layer hardened with martensite (Points 1 and 2).

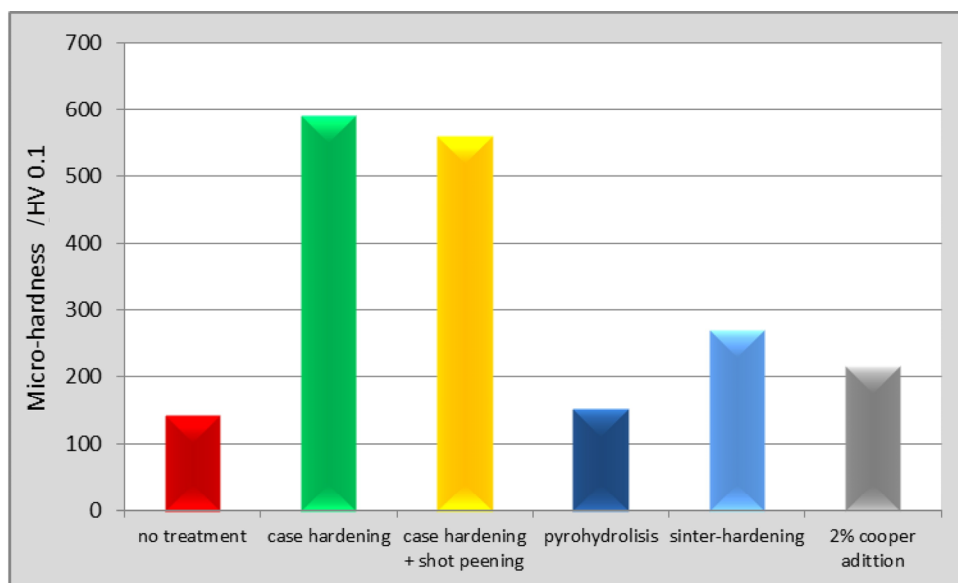


**Fig. 3** Comparison of the mean values of micro-hardness

### 3.3 E-modulus

Usually, the E-moduli of metals are determined in either tensile or compression tests. The compression test for this measurement is selected on the basis of a cuboid geometry sample with a volume of 10mm × 10mm × 15mm. The samples were taken from the gears by means of the wire EDM process. As a result, the experimental results show only a tendency, but do not provide precise results.

A sample rod is compressed by a hydraulic testing machine at a continuous speed. From the predetermined cross-sectional area and the length of the sample, the measured compressive force and the measured elongation of the sample, the E-modulus  $E$  can be calculated with the aid of Hooke's law according to Formula 3.

$$E = \frac{\sigma}{\varepsilon} \quad (3)$$

$\sigma$  Stress in N/mm<sup>2</sup>

$\varepsilon$  Elongation

The compressive force is calculated according to the following equation:

$$\sigma = \frac{F}{A} \quad (4)$$

$F$  Force in N

$A$  Surface in mm<sup>2</sup>

The relative elongation  $\varepsilon$  is calculated according to the formula 5:

$$\varepsilon = \frac{\Delta l}{l_0} \quad (5)$$

$\Delta l$  Change in length in mm

$l_0$  Original length in mm

Since up to a defined yield point the relationship between force and elongation is a linear one, one can use Hook's Law to calculate the E-modulus. The starting values for each measurement are characterised by the setting behavior of the material. For every material variant there were two measurements of the sample size.

In Table 3 one can see the comparative values of the E-moduli for the following material variants: "sinter-hardened" and "no additional treatment". Due to the hardened surface in the samples "sinter-hardened" and the resulting structural changes, its modulus of elasticity is somewhat higher than the modulus of elasticity of normal sintered gears without subsequent heat treatment. On average, this increase is 10.1%.

The E-modulus of the gears made of the material variant that has undergone "no additional treatment" reaches approximately 88% of the E-modulus of steel, while the material variant which has been "sinter-hardened" reaches 97%.

**Table 3** Comparative values of E-moduli

Material	E-modulus /N/mm <sup>2</sup>
No additional treatment	184950
Sinter-hardening	203760

### 3.4 Poisson's ratio

Poisson's ratio  $\nu$  is a dimensionless material constant that indicates how this ratio behaves in relation to the longitudinal extension of a material. It is only valid for linear elastic load cases. Typical values for steel are 0.2 to 0.33. Equation 6 describes the calculation of Poisson's ratio.

$$\nu = -\frac{\Delta d / d_0}{\Delta l / l_0} \quad (6)$$

$\Delta d$  Thickness change in mm

$d_0$  Original thickness in mm

$\Delta l$  Change in length in mm

$l_0$  Original length in mm

In order to determine Poisson's ratio, one can use the modulus of elasticity of the sample measurement. Mean values of Poisson's ratio are shown in Figure 4.

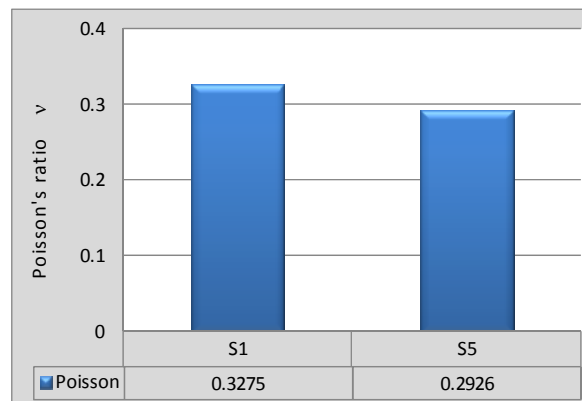


**Fig. 4** Mean values of Poisson's ratio

### 3.5 Tensile Test

With the help of a uniaxial tensile test, it is possible to determine the yield strength  $R_{p0.2}$ , the tensile strength  $R_m$ , the uniform elongation  $A_g$ , as well as the elongation  $A_5$  of any material. For this purpose, a cylindrical material sample [6] with thread at both ends was used. In the course of these experiments the material variants S1 and S5 were used. Since the samples were taken from the centre of the gear, an examination of the surface-treated materials was not possible. The diameter  $d_0$  in the centre of the sample was 3 mm. The original length  $l_0$  of the relevant sample portion equaled ten times the diameter. Figure 5 shows the tensile specimen before the test.



**Fig. 5** Tensile specimen before the test

The elongation at break and the uniform elongation can be calculated from the force and the axial strain by using the following formulae. The elongation at break  $A_5$  of the initial length  $l_0$  is related to the elongation at break of the tensile specimen. The uniform elongation  $A_g$  of the initial length  $l_0$  is related to the tensile specimen plastic elongation under stress with the maximum force.

$$A_5 = \frac{l_5 - l_0}{l_0} \cdot 100\% \quad (7)$$

$l_5$  The elongation at break of the tensile specimen in mm

$l_0$  The original length in mm

$$A_g = \frac{l_{mp} - l_0}{l_0} \cdot 100\% \quad (8)$$

$l_{mp}$  The elongation at break of the tensile specimen at maximum force in mm

The yield strength and the tensile strength can be read from the stress-strain diagram.

The six samples of material density come from three different gears of the same batch. The average values for the tensile strength  $R_m$ , the 0.2% - yield strength  $R_{p0.2}$ , the uniform elongation  $A_g$  and the elongation at break  $A_5$  are listed in Table 4.

**Table 4** Measured values of the tensile test

Designation	$R_m$ /N/mm <sup>2</sup>	$R_{p0.2}$ /N/mm <sup>2</sup>	$A_g$ /%	$A_5$ /%
S1: no additional treatment 1	395	216	11,5	13,8
S1: no additional treatment 2	389	214	11,4	12,6
S5: sinter-hardened 1	643	462	5,3	6,2
S5: sinter-hardened 2	620	440	4,8	5,1

In comparison to the wheels of the material variant S1, the wheels of the material variant S5 have a greater tensile strength by a factor of 1.61 and a smaller elongation at break by a factor of 2.38. The measurement of the elongation at break is as one should expect for sintered material, but only slightly larger than uniform elongation. This fact confirms the brittle fracture behaviour of the material used.

#### 4. Test conditions

The purpose of the tests is to simulate crossed helical gears with wheels made of different sintered steels in order to find an optimal sintered steel gear for this gear pair. The practical tests were carried out by using five test benches with a centre-to-centre distance of 30 mm. The transmission of an asynchronous motor was mounted on the test bench and the output torque was applied via a magnetic particle brake. On each test bench, an engine and a gearbox, as well as the gearbox and a brake, were connected with a gear coupling. The measurement of the output torque was made on the transmission with a torque gauge bar via a slip ring transmitter. The speeds and output torques were controlled independently for each test bench.[9,10,13] The test bench for crossed helical gears and the position of the measuring points is shown in Figure 6. The data of the test gear pair are given in Table 5.

**Table 5** Data of the test gear pair

Parameters	Data
Centre distance	30 mm
Module	1.252 mm
Transmission ratio	40
Pressure angle	20
Wheel material	Fe1.5Cr0.2Mo
Worm material	16MnCr5
Speed	1500 – 10000 min <sup>-1</sup>
Torque	12-36 Nm
Synthetic oil	Klüber GH6 1500
Mineral oil	Optigear BM 1500
Grease:	Klübersynth G34-130

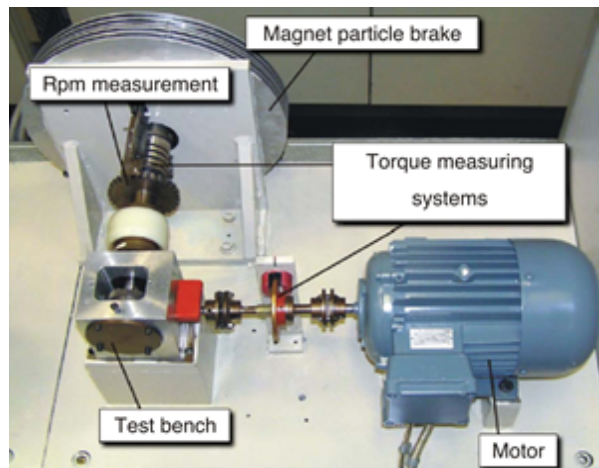


**Fig. 6** Test bench

## 5. Pitting

### 5.1 Critical damage type

For the maximum value of the transmissible torque occurring on the flanks, the following types of critical damage can be found: scuffing, wear and pitting (Fig.7). Pitting usually occurs in combination with wear and scuffing. Materials S4 (pyrohydrolysis) and S6 (2 % copper addition) were damaged by pitting when the output torque was  $T_2 = 24$  Nm, and by scuffing at the value of  $T_2 = 28$  Nm. Without any additional treatment, the S1 had the most critical wear and some pitting at the output torque of  $T_2 = 28$  Nm.

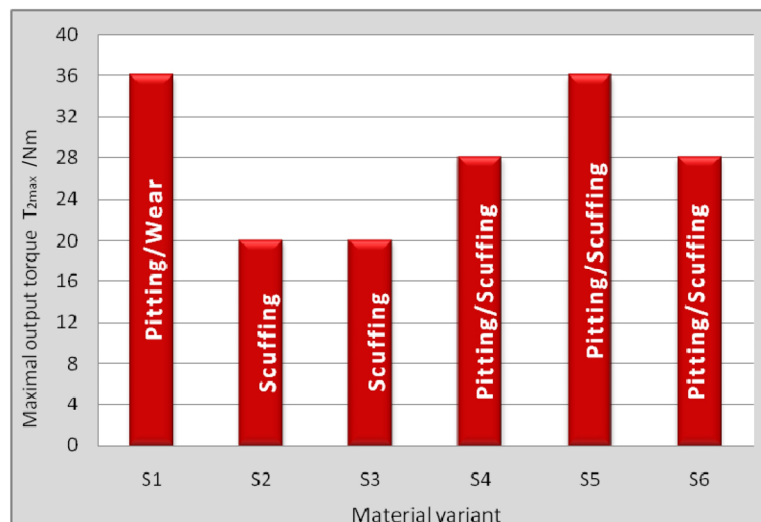


**Fig. 7** Critical damage type for different materials and input speed  $n_1 = 5000$  min<sup>-1</sup>

### 5.2 Initial pitting

A large pressure on a surface does not lead to a sudden failure of the drive, but over time small holes (pits) emerge in the shape of a shell on a tooth flank. A pit peak always points to the sliding direction. This damage occurs as a result of a cyclic fatigue due to repeated elastic and plastic deformations of the surface. The holes occur only after a

sufficiently large number of overrollings (from ca.  $5 \times 10^4$  load cycles). If merely initial pitting is present, the situation is not dangerous.

Figure 6 shows initial pitting on a tooth flank of a wheel made of material variants S1, S5 and S6. During the tests with the material S1 – no additional treatment, the initial pitting occurred under the input speed of  $n_I = 5000 \text{ min}^{-1}$  and the output torque of 36 Nm. During the tests with the material S5 – sinter-hardening, the initial pitting occurred on a wheel tooth flank under the input speed of  $n_I = 5000 \text{ min}^{-1}$  and the output torque of 16 Nm and only with mineral oil. In the material variant S6 the initial pitting occurred on a wheel tooth flank under the input speed of  $n_I = 5000 \text{ min}^{-1}$  and the output torque of 24 Nm at the number of load cycles of  $0.9 \cdot 10^6$ .

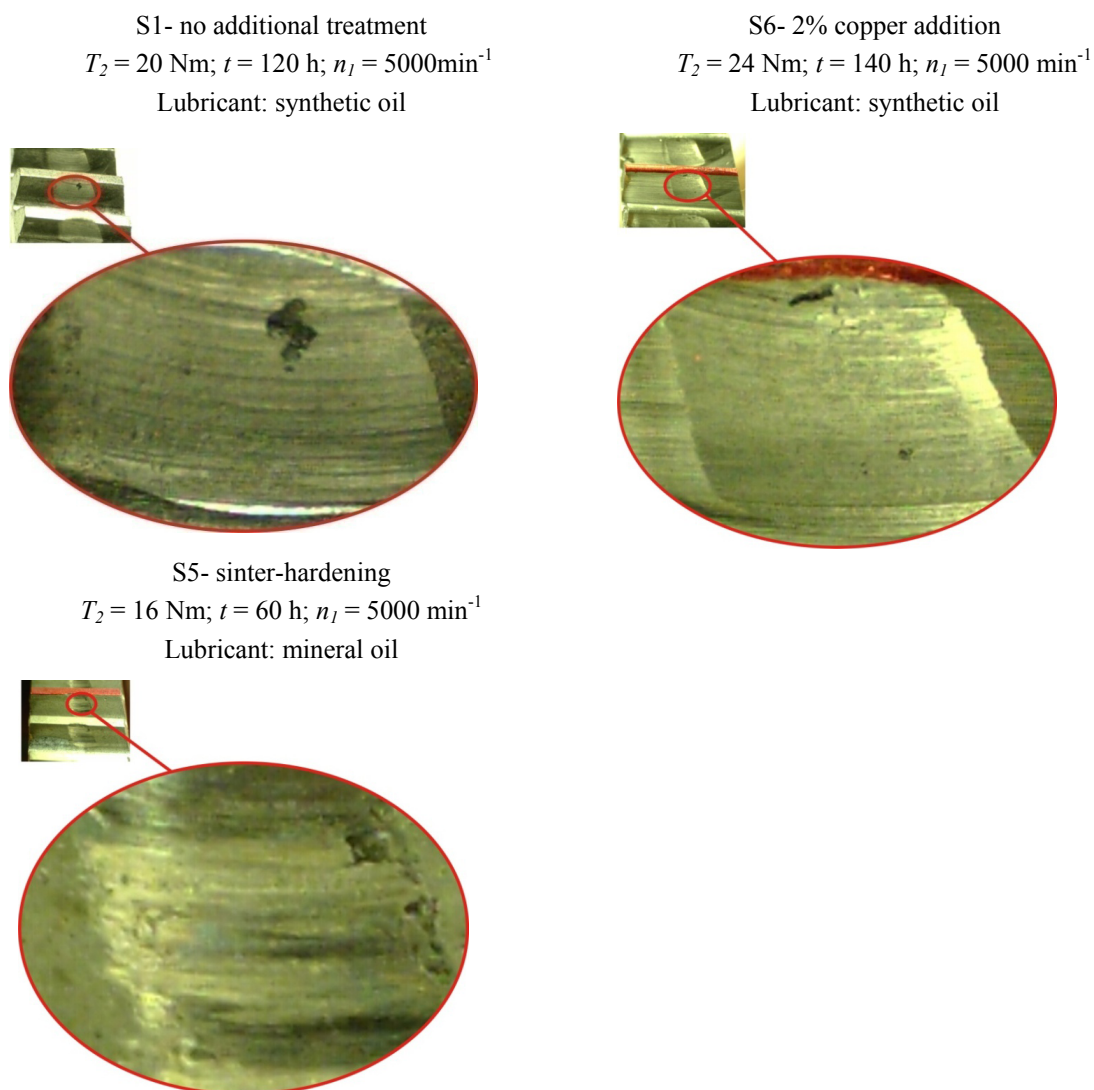


Fig. 8 Initial pitting on a wheel tooth surface made from material variants S1, S5 and S6

### 5.3 Destructive pitting

Destructive pitting destroys the flank and causes failure due to fatigue. Figure 9 shows destructive pitting on a tooth flank made of the material variants S4 and S5. During the tests with the material S4 – “pyrohydrolysis“, destructive pitting occurred after at least 160 h under the input speed of  $n_I = 5000 \text{ min}^{-1}$  and the output torque of 24 Nm. During the tests with the

material S5 – sinter-hardening, destructive pitting occurred under the input speed of  $n_1 = 10000 \text{ min}^{-1}$ . With the input speed of  $n_1 = 5000 \text{ min}^{-1}$  destructive pitting occurred on a tooth flank only when lubricating with mineral oil.

In the tests where wear volume in the tooth contact is relatively high (material S1 - no additional treatment) Hertzian pressure is reduced.[14] Therefore, in these experiments no destructive pitting occurs.

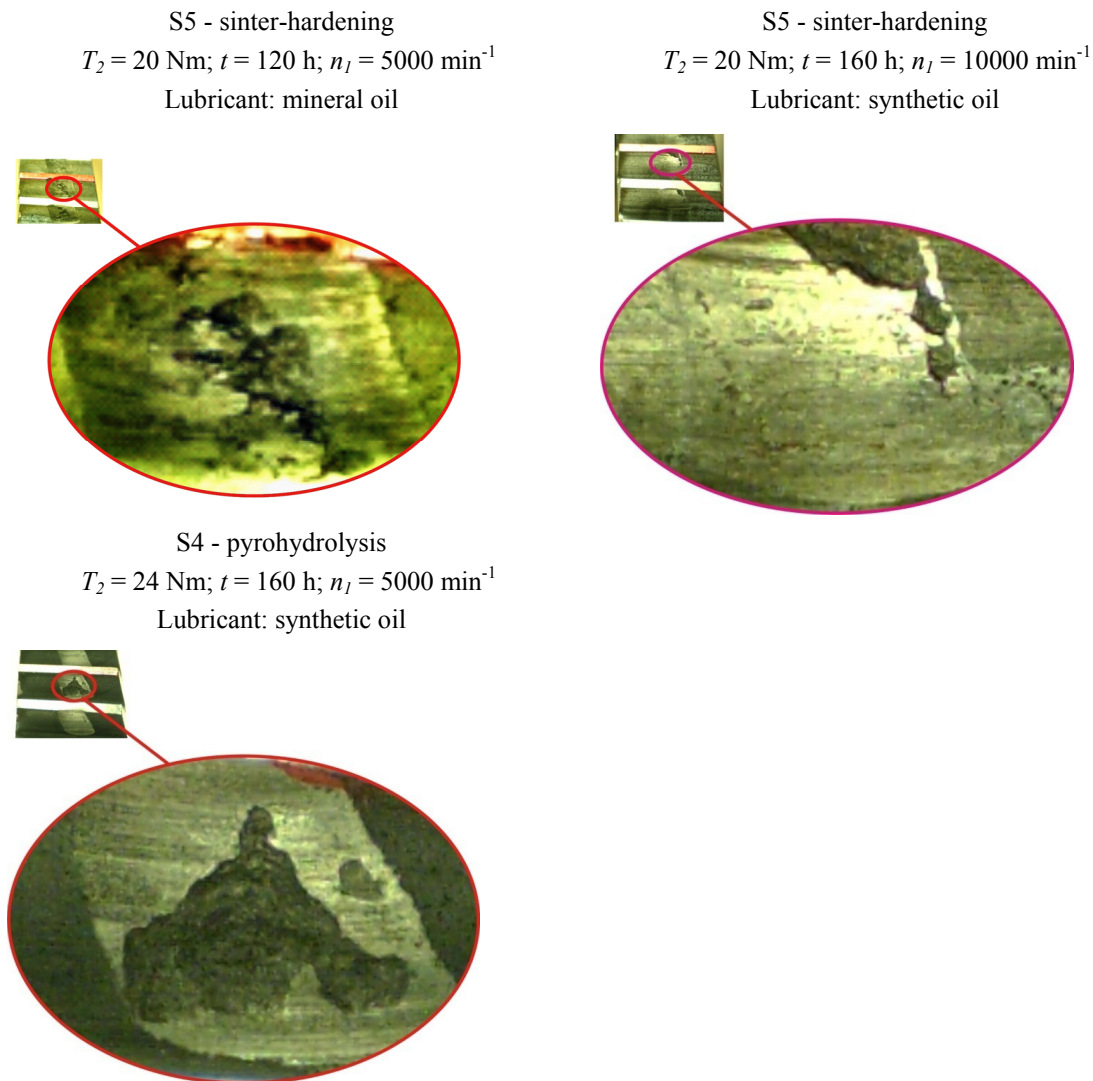


**Fig. 9** Destructive pitting on a wheel tooth flank from material variants S4 and S5

## 6. Summary

Modern technology of sintering parts has a number of advantages over the traditional method of making parts in mechanical engineering. The advantages of this technology are reflected primarily in the lower cost of production, while at the same time the quality of parts meets all the requirements of operating conditions. After producing sintered parts it is possible to carry out the final thermal treatment, which can affect the structure of the sintered steel, and thus develop high resistance to wear and pitting.

The paper presents the performed experimental research into the properties of sintered steel depending on various aftertreatments: case-hardening, case-hardening + shot peening,

pyrohydrolysis, sinter-hardening and 2% copper addition. The research has included the following material properties: chemical composition, density, hardness, E-modulus, Poisson's ratio, as well as static strength properties.

The research has shown that the material has a homogenous structure and that the composition of the alloying elements is within certain limits. The density of sintered steel is  $7.5 \text{ g/cm}^3$  which provides the sintered steel not only with good mechanical properties but also with good resistance to wear. However, one should bear in mind that the increase in density also increases the danger of pitting while the tooth contact is smaller and Hertzian pressure is higher. The lowest density of  $7.43 \text{ g/cm}^3$  is present in the following material variants: S5 - sinter-hardening and S6 - 2% copper addition.

The micro-hardness measurements have shown that the greatest hardness is found, as expected, in the material variants S2 – case-hardening and S3 – case-hardening + shot peening. The lowest hardness is found in the material variants S1 - no additional treatment and S4 – pyrohydrolysis.

The E-modulus experiment has shown that in the material variant S5 - sinter-hardening, the E-modulus reaches as far as 97% of the values of the steel E-modulus, which is satisfactory when considering the porosity of sintered steel.

The investigation into the critical damage of flanks in operating conditions showed that the most common forms of damage are pitting and scuffing. Pitting occurs in combination with other forms of damage and it can be traced in the material variants such as S1 (no additional treatment –initial pitting), S4 (pyrohydrolysis –destructive pitting), S5 (sinter-hardening –destructive pitting only when lubricating with mineral oil at  $n_1 = 5000 \text{ min}^{-1}$  and when lubricating with synthetic oil at  $n_1 = 10000 \text{ min}^{-1}$ ) and S6 (2% copper addition – destructive pitting in combination with scuffing). However, the most dangerous pitting occurs in the material variants S4 and S5 where it causes critical situation, i.e. the destruction of tooth flanks.

## REFERENCES

- [1] W. Schatt, K-P. Wieters, Pulvermetallurgie- Technologien und Werkstoffe, VDI-Verlag Düsseldorf, 1994.
- [2] T. Wendt, Tragfähigkeit von Schraubradgetrieben mit Schraubädern aus Sintermetall. Dissertation Ruhr-Universität Bochum, 2008.
- [3] S. Dizdar, P. Johansson, Höganas AB, 263 83 Höganas, Sweden: P/M Materials for Gear Application; EURO PM2007, Toulouse October 16, 2007.
- [4] W. Predki, A. Miltenović: Influence of Hardening on the Microstructure and the Wear Capacity of Gears made of Fe1.5Cr0.2Mo Sintered Steel. International Journal "Science of Sintering", 42 (2010). p. 183-191.
- [5] A. Miltenović, V. Nikolić, M. Milovančević, M. Banić: Experimental and FEM analysis of sintered steel worm gear wear. TRANSACTIONS OF FAMENA XXXVI-4 (2012), Faculty of mechanical engineering and naval architecture, ISSN 1333-1124, pp. 85-96 Zagreb 2012.
- [6] DIN EN 10002: Metallische Werkstoffe – Zugversuch, 12/2001
- [7] A. Miltenović: Verschleißtragfähigkeitsberechnung von Schraubradgetrieben mit Schraubädern aus Sintermetall, Dissertation Ruhr-Universität Bochum, 2011.
- [8] A. Miltenović, V. Nikolić, R. Mitrović: Efficiency of crossed helical gears with wheels made of sintered steel Fe1.5Cr0.2Mo with sinter-hardening treatment. TRANSACTIONS OF FAMENA XXXVI-2, Zagreb 2012.
- [9] M. Milovančević, D. Milenković, S. Troha: The optimization of the vibrodiagnostic method applied on turbo machines. TRANSACTIONS OF FAMENA XXXIII-3 (2009), Faculty of mechanical engineering and naval architecture, ISSN 1333-1124 pp. 63-71, Zagreb 2009.

- [10] M. Milovančević, J. Stefanović Marinović, B. Anđelković, A. Veg: Embedded condition monitoring of power transmission of a pellet mill. TRANSACTIONS OF FAMENA XXXIII-2 (2010), Faculty of mechanical engineering and naval architecture, ISSN 1333-1124, pp. 71-79, Zagreb 2010.
- [11] B. Anđelković, D. Milčić, D. Janošević, M. Milovančević: Modified Neural network-based study into the coefficient of friction in pressed assemblies. TRANSACTIONS OF FAMENA XXXIV-3 (2010), Faculty of mechanical engineering and naval architecture, ISSN 1333-1124, pp. 20-38 Zagreb 2010.
- [12] J. Stefanović Marinović, M. Petković, I. Stanimirović, M. Milovančević: A Model of planetary gear multicriteria optimization. TRANSACTIONS OF FAMENA XXXV-3 (2011), Faculty of mechanical engineering and naval architecture, ISSN 1333-1124, pp. 21-34 Zagreb 2011.
- [13] S. Troha, N. Lovrin, M. Milovančević: Selection of the two-carrier shifting planetary gear train controlled by clutches and brakes. TRANSACTIONS OF FAMENA XXXVI-3 (2012), Faculty of mechanical engineering and naval architecture, ISSN 1333-1124, pp. 01-12 Zagreb 2012.
- [14] A. Miltenović, V. Nikolić, M. Milovančević, M. Banić: Experimental and FEM investigation of wear of crossed helical gears. TRANSACTIONS OF FAMENA XXXVI-4 (2012), Faculty of mechanical engineering and naval architecture, ISSN 1333-1124, pp. 01-12 Zagreb 2012.

Submitted: 26.5.2014

Accepted: 10.12.2014

Mr Đorđe Miltenović  
College of Textile Leskovac  
Vilema Pušmana 17  
Dr Milan Tica  
Faculty of Mechanical Engineering  
University of Banjaluka  
Vojvode Stepe Stepanovića 71  
Dr Aleksandar Miltenović  
Dipl. Ing. Milan Banić  
Faculty of Mechanical Engineering  
University of Niš  
Aleksandra Medvedeva 14  
Mr Srđan Živković  
Faculty of Civil Engineering  
University of Niš  
Aleksandra Medvedeva 14  
Dipl. Ing. Žarko Mišković  
Faculty of Mechanical Engineering  
University of Belgrade  
Kraljice Marije 16